U.P.B. Sci. Bull., Series B, Vol. 69, No. 4, 2007 ISSN 1454-2331

CORROSION BEHAVIOUR OF CoCrMo AND CoCrTi ALLOYS IN SIMULATED BODY FLUIDS

Ioan Viorel BRANZOI[1], Mihai IORDOC[2], Mirela Maria CODESCU[3]

A fost studiată comportarea la coroziune a aliajelor Co-Cr-Mo şi Co-Cr-Ti în condiţii fiziologice simulate utilizând metode electrochimice. Au fost obţinute potenţialul în circuit deschis (OCP) (după 2 ore), curbele de polarizare potenţiodinamice (PPC) (într-un domeniu de potenţial de la -1500 mV la + 1500 mV, SCE), variaţia în timp a rezistenţei la polarizare (100 de valori ale rezistenţei la polarizare), spectroscopia electrochimică de impedanţă (EIS) (10^5 – 10^{-3} Hz, la potenţialul în circuit deschis). Spectrele EIS (10^5 – 10^{-3} Hz) au prezentat un sistem cu o singură constantă de timp sugerând formarea unui strat de oxid (film de oxid monostrat) pe suprafaţa metalului. Toate măsurătorile au fost efectuate în soluţie Hank aerată la 37±0,2ºC. Comportarea electrochimică a aliajelor a fost diferită. Rezistenţa la coroziune a aliajului Co-Cr-Mo a fost mai mare decât în cazul aliajului Co-Cr-Ti, iar stabilitatea filmului pasiv de oxid este mai mare în cazul aliajului Co-Cr-Mo.

The corrosion behaviour of CoCrMo and CoCrTi alloys under simulated physiological conditions was investigated using the electrochemical methods. Thus, the open circuit potential (OCP) (for two hours), potentiodynamic polarization curves (PPC) (within a potential range of -1500 to +1500 mV/SCE) and time variation of polarization resistance (100 polarization resistance values) were obtained. The electrochemical impedance spectroscopy (EIS) spectra exhibited a one-time constant system, suggesting the formation of a one-layer oxide film on the metal surface. All measurements were carried out in Hank's aerated solution at 37 ± 0.2 ^{0}C. The electrochemical behaviour of the alloys was different. The corrosion resistance of Co-Cr-Mo alloy was higher than in the case of Co-Cr-Ti alloy, and the stability of passive oxide film is higher in the case of Co-Cr-Mo.

Keywords: corrosion, CoCrMo, CoCrTi, Hank's solution, EIS.

[1] Prof., Dept. of Applied Chemistry and Materials Science, University "Politehnica" of Bucharest, Romania
[2] Eng., National Institute for Research and Development in Electrical Engineering, Bucharest, Romania
[3] Eng., National Institute for Research and Development in Electrical Engineering, Bucharest, Romania

1. Introduction

The CoCr alloys, developed several decades ago for the aerospace industry, also achieve their inertia through the formation of a chromium oxide surface layer. They have excellent mechanical properties and are widely used in orthopedic implants. The alloys are generally CoCrMo or CoNiCrMo, and may also include other elements such as tungsten or iron (Fe). Apart from the fact that Ni can be avoided in the formulation, CoCr alloys have advantages over stainless steel in terms of better corrosion resistance and somewhat better mechanical properties for certain applications.

Both wrought and cast CoCr alloys are used in prosthetic devices, each version having distinct properties. They are often used as components in modular prosthetic devices such as hip or knee joints, being the most suitable for bearing surfaces (often against ultra-high-molecular-weight polyethylene) [1-5].

Load bearing medical implants such as the hip and knee joints undergo highly variable loading in an aggressive physiological environment. The implant materials are required to have appropriate mechanical, physical, chemical and biological properties. Co-Cr alloys, which have excellent corrosion resistance, wear behaviour, and biocompatibility, are amongst the few materials which can fulfill these requirements [6,7]. The quality of Co-Cr castings has been improved thanks to advances in manufacturing techniques over the years. However, rare incidences of fracture still occur in service. Scanning electron microscopy has revealed extensive facets on the fatigue fracture surface and zig-zag shaped secondary cracking on the adjacent fracture surface. The matrix of the Co-Cr alloy has a face centered cubic (fcc) structure and it would be expected that crack propagation occurs along {111} planes, e.g. in Ni-based alloys, such planes are the main slip planes for deformation at low temperature [8]. In studies of failure in Co-Cr alloys, crack propagation along these planes has been suggested to occur [9], but crystallographic evidence for this is lacking [10].

Considering that CoCr alloys and titanium belong to a few metallic materials which fulfill the strong requirements for corrosion resistance and biocompatibility, the good performances for CoCrTi alloys can be expected. The available data confirm that the addition of titanium to CoCr alloy can improve some mechanical and physical properties [11,12], but on the other side they show insufficiency in the investigation of this topic. Therefore, the purpose of this study was to prepare and investigate some selected CoCr alloys as potential for biomedical application [13].

2. Experimental

The investigated alloys were: Co76-Cr20-Ti4 and Co-Cr-Mo (at. %). First alloy was prepared by melting in induction furnace and the second alloy was a commercially alloy (Beznoska Co. Czech Republic).

A VoltaLab 40 model electrochemical combine with dynamic EIS (Electrochemical Impedance Spectroscopy) was used for the electrochemical polarization. The polarization behaviour of Co-Cr alloys was studied in a classical electrolytic cell with three electrodes. A platinum plate electrode and a saturated calomel electrode (SCE) were used as counter and reference electrode respectively. All three electrodes (including working electrode) were placed in a cell which has been connected to a UltraThermostat type U10 with external recirculation of heating water to maintain the temperature inside the cell close to 37 ^{0}C. Samples with 1 cm^2 geometric surface area were used. Prior to experiments, the electrodes were polished with SiC emery paper down to #4000. After polishing, the electrodes were degreased in acetone, washed with Millipore water and then introduced into the measurement cell. The working electrode potential was scanned on the potential range of -1000 mV up to +1200 mV/SCE with scan rate of 0.5 mV/sec. This scan potential range was chosen taking into account that, the potential – pH diagram for physiological conditions generally showed that, the potential value of a metallic biomaterial may vary from -1.0 to +1.2 V/SCE in the human body. Excellent reproducibility was achieved when a potentiostatic reduction was applied for 10 minutes. The corrosion current density (i_{corr}) was determined by extrapolation of the anodic and cathodic curves in the Tafel potential range.

The open circuit potential (OCP) and the polarization resistance measurements were carried out for 2 hours (in case of OCP), and for polarization resistance measurements was determined 100 points at anodic and cathodic polarizations of ± 60 mV/SCE, around of stationary potential.

Impedance measurements were performed using VoltaLab 40 dynamic EIS with VoltaMaster 4 Software on the frequency range between 100 kHz and 1 mHz with an AC wave of ± 5 mV (peak-to-peak) overlaid on a DC bias potential and the impedance data were obtained at a rate of 10 points per decade change in frequency.

All tests have been performed in Hank solution (Table 1) at 37 ± 0.2 ^{0}C under atmospheric oxygen conditions without agitation.

3. Results and Discussion

The OCP type measurement for the Co76-Cr20-Ti4 alloy, presented in Fig. 1, showed that in Hank solution, the stationary potential decreases in the first

time period and then increases to more electropositive values and tends to a limit value.

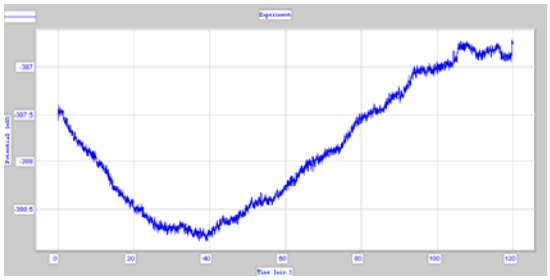

Fig. 1. The OCP versus time for Co76-Cr20-Ti4 alloy in Hank solution

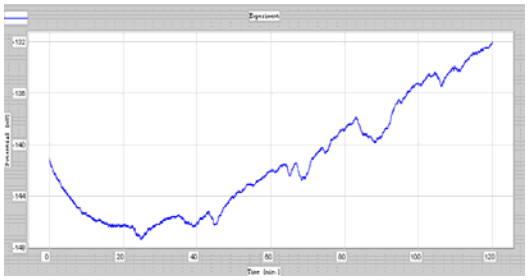

Fig. 2. The OCP versus time for Co-Cr-Mo alloy in Hank solution

Similarly, the Fig. 2 presents the stationary potential evolution in time for the Co-Cr-Mo alloy samples in the Hank solution. Analyzing in comparison the Figs. 1 and 2 it can be observed the same behaviour of both alloys and in this case the stationary potential decreases at the initial stage and then increases to more electropositive values of potential, like in case of the Co76-Cr20-Ti4 alloy samples.

Figs. 3 and 4 present the evolution of polarization resistance in time for the Co76-Cr20-Ti4 alloy and Co-Cr-Mo samples in Hank solution. Polarization resistance increases in time, which means that a passive oxide film was formed on the electrode surface, which makes the charges transfer more difficult.

Fig. 5 presents the polarization curve, obtained by potentiodynamic method, by scanning the working potential electrode in a potential range of -2000 ... + 3000 mV/SCE for the Co76-Cr20-Ti4 alloy samples in Hank solution with a potential sweep rate of 0.5 mV/s. Two characteristic zones can be observed at cathodic branch, one related to the reducing of the dissolved oxygen in the electrolyte, followed by the hydrogen evolution. At the anodic polarization curve, after a first anodic dissolution domain, it can be observed a first passivity range from +200 to +700 mV which correspond to a primary low-stable oxide layer formation, followed by a transpassive region and a second passivity range, which starts at ~ +2000 mV and corresponds to a passive oxide stable film formation.

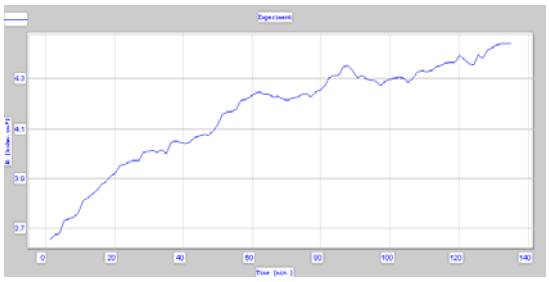

Fig. 3. The polarization resistance versus time for Co76-Cr20-Ti4 alloy in Hank solution

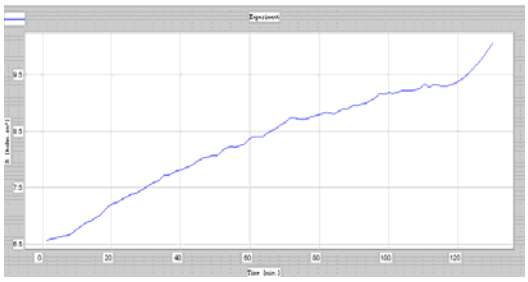

Fig. 4. The polarization resistance versus time for Co-Cr-Mo alloy in Hank solution

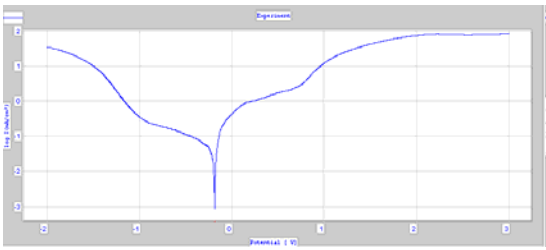

Fig. 5. Polarization curve for Co76-Cr20-Ti4 alloy in Hank solution

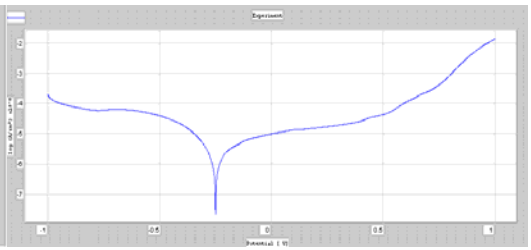

Fig. 6. Polarization curve for Co-Cr-Mo alloy in Hank solution

The extrapolation Tafel method was used for the low overvoltages domain and in this mode were obtained the corrosion parameters which are given in Table 2.

Fig. 6 presents the anodic and cathodic polarization curves for the Co-Cr-Mo alloy samples in Hank solution, in a potential range of -1000 mV/SCE…+1000 mV/SCE. Like in the case of Co76-Cr20-Ti4 alloy, working electrode potential was scanned with a potential sweep rate of 0.5 mV/s. Analyzing the Fig. 6 it can be observed that on the cathodic curve appear two distinct processes, corresponding to the reduction of the electrolyte dissolved oxygen and hydrogen evolution. On the anodic curve it can be observed a first anodic dissolution domain, followed by a passive potential range which indicates the formation of an intermediary passive film, less stable, consisting from non-stoechiometric Co oxides and of alloying elements, and a transpassive potential range where the current increases slowly, and this increasing is due to the oxygen evolution.

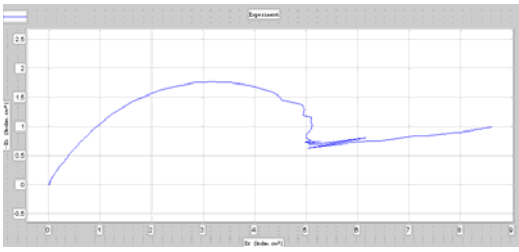

Fig. 7a. Nyquist diagram for Co76-Cr20-Ti4 alloy in Hank solution

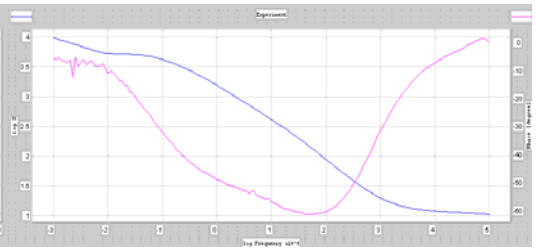

Fig. 7b. Nyquist diagram for Co76-Cr20-Ti4 alloy in Hank solution

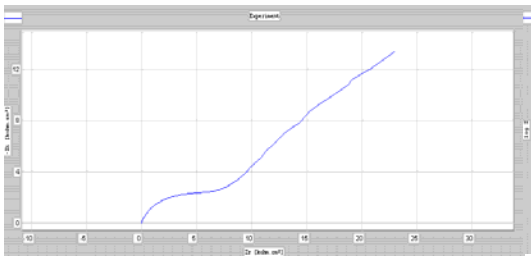

Fig. 8a. Nyquist diagram for Co-Cr-Mo alloy in Hank solution

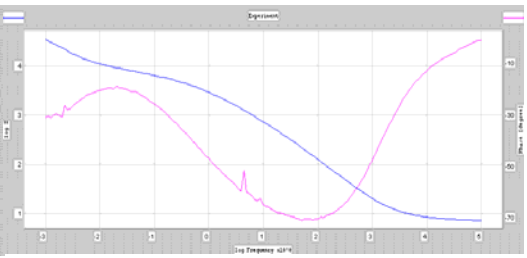

Fig. 8b. Bode diagram for Co-Cr-Mo alloy in Hank solution

The EIS measurements were carried out at open circuit potential (OCP) after 10 minutes of immersion. Analyzing the Nyquist diagram for Co-Cr-Ti alloy (Fig. 7a) it can be observed that at high frequencies appears a capacitive loop very well defined, which is followed by a inductive-diffusive branch at medium and low frequencies. This behaviour is pointed out by the Bode diagram (Fig. 7b). As we can see from Bode diagram on the phase angle vs. log frequency curve appears a maximum very well defined that correspond at the phase angle of 60^0, that means a capacitive with diffusive tendencies behaviour of Co-Cr-Ti electrode in this environment.

In Fig. 8a are presented the Nyquist diagrams for the Co-Cr-Mo alloy. Analyzing this Fig. it can be observed that, the Nyquist diagram presents a very high and wide capacitive loop at high and medium frequencies followed by a diffusive region. This behaviour is pointed out by the Bode diagram (Fig. 8b). As we can see from the Bode diagram on the phase angle vs. log frequency curve appears a maximum very well defined that correspond at the phase angle of approximately 75^0, that means a capacitive behaviour of the Co-Cr-Mo electrode in this environment. This behaviour points out that on the Co-Cr-Mo electrode surface a stable oxide film is formed, which hinders the charge transfer reaction, and is in accordance with the potentiodynamic polarization behaviour.

The values of electrochemical parameters obtained from Nyquist and Bode diagrams are presented in Table 3.

Table 1

Chemical composition of simulated body fluid

Electrolyte	Composition
Hank's solution	NaCl 8 g/l ; $CaCl_2$ 0,14 g/l ; KCl 0,4 g/l ; $MgCl_2*6H_2O$ 0,1 g/l ; $Na_2HPO_4*2H_2O$ 0,06 g/l ; KH_2PO_4 0,06 g/l ; $MgSO_4*7H_2O$ 0,06 g/l ; glucose 1 g/l

Table 2

Electrochemical parameters obtained from polarization curves

Sample	E_{cor}, mV	i_{cor}, µA/cm^2	b_a, mV/dec	b_c, mV/dec	P, µm/year	R_P, kohm*cm^2
Co-Cr-Ti	-304	2.8091	161.3	-126.4	21.34	8.72
Co-Cr-Mo	-250.3	1.3434	178.4	-104.5	10.2	16.54

Table 3

Electrochemical parameters obtained from Nyquist and Bode diagrams

Sample	R_{el}, ohm*cm^2	R_P, kohm*cm^2	C, µF/cm^2	Time constants		
				ω, Hz	log |Z|, kohm*cm^2	-Phase, degree
Co-Cr-Ti	5.04	6.371	249.8	1.701	1.02	60
Co-Cr-Mo	-4.8	6.785	83.5	1.832	0.8706	75

4. Conclusions

The potentiodynamic polarization curves showed that, in all the cases, the working electrode was directly translated to a stable passive behaviour from the Tafel region without exhibiting an active-passive transition.

Co-Cr alloys have a passive behaviour on a large potential range. At more positive potentials, the current densities increase again, due to both transpasivation and oxygen evolution reaction.

In Hank solution at 37 ^{0}C the lowest value of the corrosion current density is for Co-Cr-Mo alloy for which was obtained the highest value of polarization resistance. The addition of the alloying elements such as Ti, led to the decrease of corrosion resistance of this metallic biomaterial in Hank solution.

The EIS measurements were used to characterize the semi-conductive properties of the oxide films. The Nyquist and Bode diagrams were plotted at the open circuit potential. The obtained Bode diagrams were in good accordance with the Nyquist diagrams, confirm the superiority of the Co-Cr-Mo alloy.

R E F E R E N C E S

[1] *N. Gibson, H. Stamm*, The Use of Alloys in Prosthetic Devices, report in Medical Device Manufacturing & Technology, 2002.

[2] *I. Gotman*, Characteristics of Metals Used in Implants, J. of Endourology, 11 (1997) 6, 383-389.

[3] *L. Shi, D.O. Northwood*, The properties of a Wrough Biomedical Cobalt-Chromium Alloy, J. Mater. Sci., 29 (1994) 1233-1238.

[4] *M. Niinomi*, Recent Metallic Materials for Biomedical Applications, Metall. Mater. trans., 33A (2002) 477 – 486.

[5] *L. Reclaru, R. Lerf, P.-Y. Eschler, J.-M. Meyer*, Corrosion Behaviour Of Metallic Surgical Implant Rex 734 - Cocr; Pitting, Crevice And Galvanic Corrosion Evaluation, European Cells and Materials **Vol. 1**. Suppl. 1, 2001 (pages 29-30)

[6] *Browne M. & Gregson, P.J.* (2001) Accelerated fatigue testing of knee tibial trays. DTI CAM 2 Project Task 5, University of Southampton

[7] *Chen, J., Browne, M., Taylor, M., Gregson, P.J.* (2004) Application of an interface failure model to predict fatigue crack growth in an implanted metallic femoral stem. Computer methods and programs in biomedicine. 73, 249-256.

[8] *Reed, P.A.S., Wu, X.D., & Sinclair, I.* (2000) Fatigue crack path prediction in UDIMET 720 nickel-based alloy single crystals. Metall. Mater. Trans. A 31, 109-123.

[9] *Zhuang, L.Z. & Langer, E.W.* (1990) Effects of alloy additions on the fatigue properties of cast Co-Cr-Mo alloy used for surgical implants. J. Mat. Sci. 25, 683-689.

[10] *S. C. Wang, M. Browne, H. S. Ubhi, M. J. Starink* Determination of the fatigue fracture planes of Co-Cr-Mo biomedical alloys using electron backscatter diffraction, *Journal of Microscopy 217(2005)118-121*.

[11] *V.D. Rudiger, A. Hoffman, D. Hirschfeld,* Eine neue titanhaltige kobalt-chrom dentallegierung, Dent. Labor (Munch), 18 (1970) 24-31.

[12] *Y. Igaqrashi,* Cobalt-Chrome-Titanium Alloys Dentitan, Features and Physical Properties, J. Dent. Technol., 13 (1985) 15-21.

[13] *LJ. Slokar et al.,* Microstructures and Hardness of CoCrTi Alloys for Dental Castings, Metalurgija 43 (2004) 4, 273 – 277.